Neutron and synchrotron studies of structure and magnetism of Shape Memory Alloys

J. M. Barandiarán[1]*, V. A. Chernenko[1,2], P. Lázpita[1], J. Gutiérrez[1], M. L. Fdez-Gubieda[1] and A. Kimura[3]

[1] BCMaterials and University of the Basque Country (UPV/EHU), Leioa , Spain
[2] Ikerbasque, The Basque foundation for Science, Bilbao, Spain
[3] Graduate School of Science, Hiroshima University, Hiroshima, Japan

*manub@we.lc.ehu.es

Abstract. Magnetic Shape Memory Alloys have attracted a large interest from the basic aspects of their structural and magnetic transitions, as well as from their possible technological applications as very rapid, contactless, high stroke actuators. The typical alloy composition for such materials is Ni-Mn-X (X= Ga, In, Sb, Sn, etc.). The electronic and magnetic structure of such alloys are on the base of the displayed properties and are object of intense study by all kind of advanced experimental and theoretical methods. Here we present a summary of recent diffraction experiments with neutron, X ray Magnetic Circular Dichroism (XMCD) and X ray Photoemission Spectroscopy (XPS) that are complementary to elucidate the electronic and magnetic character of these alloys and the changes occurring at the martensitic transformation. While rigid band models can account for most electronic features, magnetism is better described by a localized moment mainly concentrated at the Mn atoms.

1. Introduction: Magnetic Shape Memory Alloys, neutrons and synchrotron

Magnetic Shape Memory Alloys (MSMA), with typical compositions Ni-Mn-X (X= Ga, In, Sb, Sn, etc.) have raised large interest during the last years, due to their multifunctional properties. Such properties are based on the ferromagnetic thermoelastic Martensitic Transformation (MT) that produces a multivariant martensitic phase. Martensites have complicated crystallographic and magnetic structures [1-3]. The martensitic and accompanying transitions are also complex; it involves phonon softening modes mechanisms and can end in several modulated and non-modulated structures, very sensitive to the exact composition of the alloys. Such structures are sometimes mixed up in a given alloy. Different degrees of order among the different atomic species can also be present in the same sample and evolve as a function of time and annealing. In addition, different magnetic atoms are involved in the magnetism. For instance, the prototype stoichiometric Heusler compound Ni_2MnGa, and off stoichiometric NiMnGa alloys, the most studied ones, have localized 3d magnetic moments linked to Mn and Ni atoms, with possible ferro and antiferromagnetic contributions to the coupling [4, 5]. Probably some itinerant contribution related to s electrons, shared by all components, is present too.

MSMA have been studied by X rays, TEM, synchrotron radiation and neutron techniques [2, 3, 6-9]. Neutron diffraction is a well-established technique for crystal and magnetic structure studies. As compared with X-ray and electron diffraction, it presents a number of advantages, like: a) the nuclear interaction is described by point like potentials [10, 11]. Scattering from neutrons gives a special

sensitivity to large diffraction angles because do not depend on the scattering angle. b) Neutron scattering factors are not proportional to the atomic number, as in x-rays and electrons, and can even be negative, so that there can be a large contrast between neighbor elements (figure 1). c) Neutron penetration in matter is very large as compared with x-rays and electrons and bulk samples can be fully explored by neutrons, in contrast with near surface analysis by the other techniques. Also especial equipment, as cryostats and furnaces or superconducting magnets, can be employed with little perturbation of the beam and diffraction pattern. d) Neutrons are sensitive to the magnetic moment of the atoms and are invaluable to study magnetic structures. e) Neutron mass is similar to the atomic one so the inelastic interaction with matter, Inelastic Neutron Scattering (INS), can excite phonons and magnons which are difficult to observe with other types of radiation.

Neutrons also have some issues as: a) Neutrons studies need a large amount of sample. At least one gram is required for efficient powder diffraction data acquisition. b) There is no direct interaction with the electronic structure of the solid.

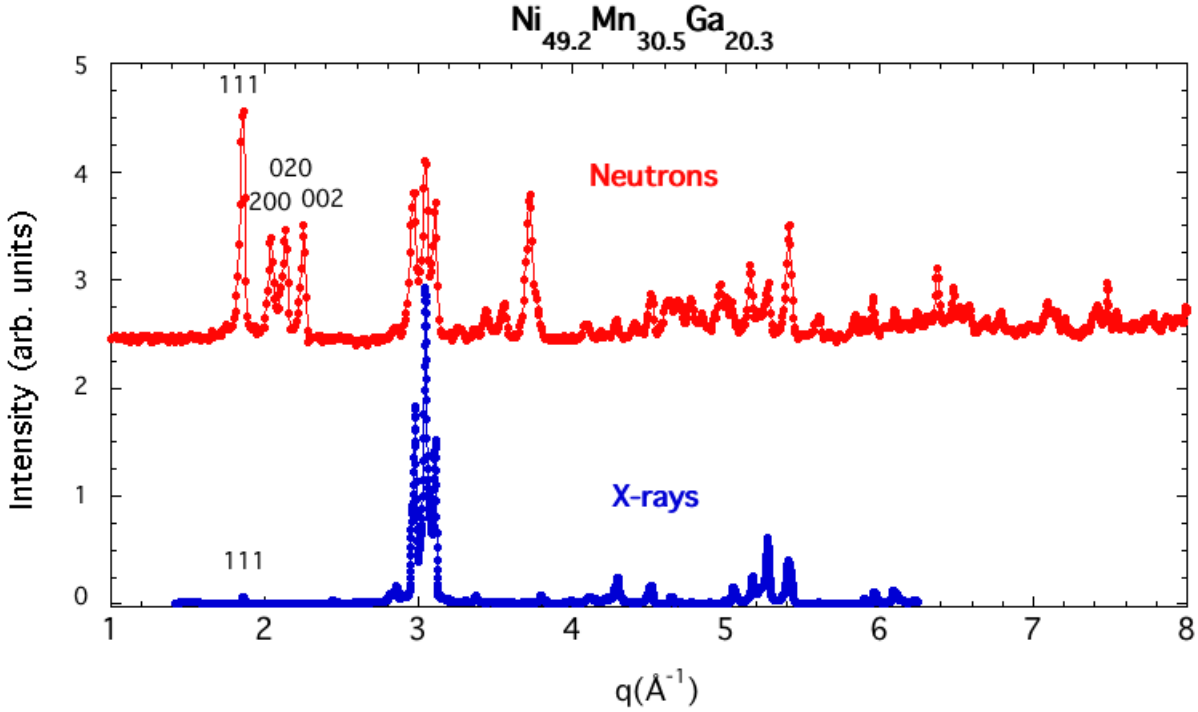

Figure 1. Comparison between X-rays and neutron diffraction patterns in a Magnetic Shape Memory Alloy. Note the intense superstructure peaks in the neutron diffraction are absent in the X-rays. Neutron intensity at large scattering angles are much more intense as well.

The synchrotron radiation is in fact complementary to neutrons for it is so strong that minute samples can be used with full resolution and large signal to noise ratio. Strong interaction with electrons provide data about the electronic structure too. Moreover, X-ray Magnetic Circular Dichroism (XMCD) provides atom selective magnetic information that complements the site selective information of neutrons.

In this paper we present a short survey of scattering experiments with neutrons, as well as X ray Photoemission Spectroscopy (XPS) and XMCD, which are complementary to elucidate the electronic and magnetic character of MSMA and the changes occurring at the martensitic transformation.

2. INS and XPS at the Martensitic transition

The Martensitic transformation has a number of possible final states including modulated structures extending over 5 or 7 lattice cells. In the prototype is the stoichiometric Ni_2MnGa, there is a pre-martensitic transformation that frozen the modulated structure in the cubic lattice, before the Martensitic

transformation to a tetragonal L21 phase takes place. The "premartensitic" transformation from the cubic parent phase leads to a near-cubic modulated intermediate phase by means of of a soft phonon mode mechanism. A Zehludev, SM Shapiro et al. studied this transition using Inelastic Neutron Scattering (INS) in the 90's [12]. Recently V. Recarte, J. I. Pérez-Landazabal et al. [13] have shown the role of the magnetoelastic coupling in the transformation using inelastic neutron scattering under magnetic field. The experiment shows a temperature shift of the characteristic energy dip of the transverse acoustic branch TA2 under the magnetic field. Determination of the phonon dispersion relationship is a typical Neutron task and gives a deep insight into the mechanism of the martensitic transition and the modulation effects.

On the other hand, it has been proposed early in the study of MSMAs, that the main parameter driving the martensitic transformation and magnetic properties of FSMA is the electron concentration or average number of valence electrons for atom (e/a) so the electronic structure can be a key for the interpretation of the stability of some alloys that do not transform. The electronic structure of FSMAs, or at least their density of states (DOS), can be determined by X-ray Photoemission Spectroscopy (XPS), which is a technique available in many laboratories. Soft X rays, however, can only probe a few atomic distances from the surface of the material. To get a deeper probe, representative of the bulk, we need high energy X-rays and, therefore, a synchrotron source is essential.

In this way, XPS experiments at high energy (8keV) have been performed recently in Spring 8 onto two different NiMnGa samples with large differences in their electron concentration, so the low e/a alloy does not show the martensitic transition (MT) [14]. The following findings were obtained from the experiments:

- The spectral weight near EF is larger for larger e/a
- Ni 3d eg peak shifts to higher energy by 0.2 eV upon MT
- Rigid band model is not applicable for different e/a
- Jahn-Teller distortion scenario explain the MT al high e/a
- For low electron concentration, the electron energy gain in the split band is not sufficient to overcome the energy loss from the lattice distortion and no MT occurs.

3. Preferential site occupancy and magnetic moment

Electron concentration can be taken as the main parameter driving transformation and magnetic properties of FSMAs as a first approximation. However, in off stoichiometric alloys the magnetic moment is not a single function of e/a but the exact distribution of magnetic atoms in the lattice must be taken into account. For instance, the increase of order upon annealing in a rapidly quenched MSMA ribbon induces the corresponding increase of the magnetization (34%), martensitic transformation (>10K) and Curie temperature (>20K) [15], so that an alloy with different atomic order has different transformation and magnetic properties. The evolution of chemical order upon annealing in MSMAs has been studied by Recarte et al. [16] using neutron diffraction experiments. Another technique that allows changes in atomic order to be followed is EXAFS. This was applied to the rapidly quenched ribbon already mentioned with composition Ni51Mn28Ga21 by Chaboy et al. [17]. Measurements were carried out at Spring 8 in Japan.

The radial distribution function (RDF) around Mn and Ni atoms are shown in fig.2 in the as quenched state and after annealing. This function is obtained as the Fourier transform of the EXAFS function obtained in the K absorption edge, and reflects the atomic distribution around a given atom. It is clear that the Ni atoms have its neighborhood unchanged by the annealing while the Mn atoms undergo a drastic change that correspond to an ordering process reflected in the higher amplitude and lower width of the RDF. This indicates that the ordering process leaves the Ni atoms unchanged but Mn ones reorganize and lower the randomness around them.

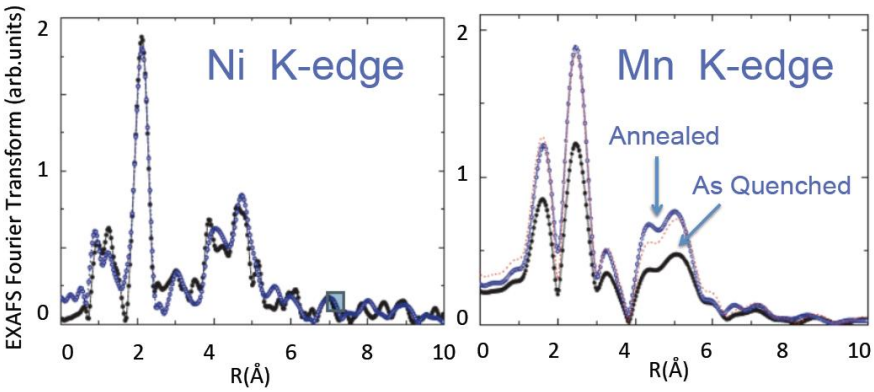

Figure 2. Radial distribution function around Ni and Mn atoms in a rapidly quenched ribbon of composition $Ni_{51}Mn_{28}Ga_{21}$, both as quenched and after 18 hours annealing at 315 ºC. The Mn atoms undergo a clear reorganization but Ni ones remain unchanged.

Another interesting feature is the distribution of excess atoms among the vacant sites in off-stoichiometric alloys. In order to determine the preferential site occupancy as a function of the composition, neutron diffraction experiments have been carried out in a series of NiMnGa alloys. The experiments were performed at the high flux diffractometer D20 at the Institute Laue Langevin (ILL) in Grenoble, France. Main results are summarized in table 1. More details are given in [18,19].

Table 1. Site occupation of the atoms in the studied alloys, as deduced from the neutron diffraction experiments. The Wyckoff nomenclature is used together with the most simple one related to the atoms that occupy the site in the stoichiometric Ni2MnGa alloy.

Site (Wyckoff)	$Ni_{44}Mn_{38}Ga_{18}$			$Ni_{49}Mn_{31}Ga_{20}$			$Ni_{50}Mn_{29}Ga_{21}$			$Ni_{52}Mn_{26}Ga_{22}$		
	Ni	Mn	Ga	Ni	Mn	Ga	Ni	Mn	Ga	Ni	Mn	Ga
Ni (8c)	1.79	0.21	0.0	1.97	0.03	0.0	2.0	0.0	0.0	2.0	0.0	0.0
Mn (4a)	0.0	1.0	0.0	0.0	1.0	0.0	0.0	1.0	0.0	0.08	0.92	0.0
Ga (4b)	0.0	0.25	0.75	0.0	0.19	0.81	0.0	0.16	0.84	0.0	0.12	0.88

The following conclusions can be drawn: For alloys with Mn excess and defect of Ni and Ga, the Mn excess occupies the Ni and Ga vacant positions. In those alloys with both Ni and Mn excess, the Ni atoms go to Mn positions, displacing properly sited Mn atoms to Ga positions.

Now we can try to apply a localized magnetic moment model based on the early values of the moment obtained in the stoichiometric alloy Ni2MnGa by J Brown et al. [2] and Islam et al. [20]. The main assumptions of our model are:

a) The magnetic moment of the alloys is localized. Mn has 3.51μB and Ni 0.33μB
b) Mn atoms couple ferromagnetically (FM) when located at proper sites
c) Mn atoms at shorter distances have antiferromagnetic (AF) interactions
d) Ni always couple ferromagnetically to proper sited Mn
e) Coupling between off site Mn atoms is given by the Bethe Slater curve (Fig. 3)

The above model allows to calculate the average magnetic moment of any alloy, if the site occupancy is known. As depicted in fig. 3 we assume AF coupling between MnMn and MnGa atoms in excess Ni alloys. In defect Ni alloys, however, the Ni positions occupied by Mn atoms have the strongest AF coupling with MnMn ones, so that they can upturn the AF coupling between adjacent MnMn and MnGa atoms to FM. Taking into account the above considerations we obtain the magnetic moment values in

table 2. They show a much better agreement with experimental values than the predictions of the rigid band model, also included for comparison.

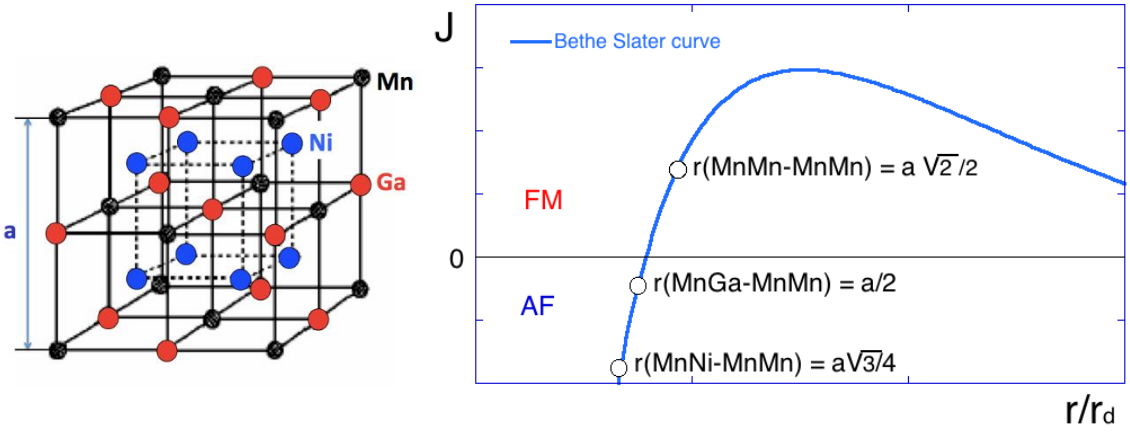

Figure 3. L21 crystal structure of Ni_2MnGa in the austenitic phase and exchange interactions between Mn atoms at different sites of the structure, assuming Bethe-Slater exchange variation with distance.

Table 2. Experimental and calculated moments of some studied alloys. All moments are given in Bohr magnetons (μ_B) per formula unit. e/a = electron concentration; μ_{EXP} = experimental moment determined at 5 K; μ_{RB} = calculated moment in the Rigid Band model; μ_{LOC} = calculated moment in the localized model.

Alloy	e/a	μ_{EXP}	μ_{RB} (error)	μ_{LOC} (error)
$Ni_{44}Mn_{38}Ga_{18}$	7.58	3.06	2.37 (22.4%)	2.96 (3.3%)
$Ni_{49}Mn_{31}Ga_{20}$	7.67	3.41	3.39 (0.6%)	3.46 (1.5%)
$Ni_{50}Mn_{29}Ga_{21}$	7.67	3.60	3.60 (0.1%)	3.55 (1.2%)
$Ni_{52}Mn_{26}Ga_{22}$	7.68	3.59	4.02 (12.0%)	3.48 (3.1%)

4. Direct determination of the magnetic moment

While the above model, together with the determination of site occupancy of the different magnetic atoms, gives quite good values for the total magnetic moment of the studied alloys, several points, as the possible contribution of conduction electrons to the magnetic moment, remain unclear and the most direct determination of the magnetic moment at each crystallographic site is welcome. For this to be achieved, polarized neutron scattering (PNS) in single crystals is a perfect tool.

PNS has been recently performed in single crystals of compositions $Ni_{52}Mn_{26}Ga_{22}$, $Ni_{49}Mn_{30}Ga_{21}$ and $Ni_{43}Mn_{38}Ga_{19}$, grown by the Bridgman method at the Ames Laboratory (Iowa, USA) [21]. The compositions are almost isoelectronic, but cover a quite large range of Ni concentrations as to be representative for testing the previous localized moment model. The nuclear structure of the alloys was determined at the ILL on D10 and D15 instruments. Polarized neutron diffraction measurements were carried out at D3 in the austenitic phase. Data analysis was performed using flipping ratios fits with the FullProf software. Maximum Entropy method [22] MemSys code, available at the ILL, was used for direct visualization of the atomic magnetization density maps using the Fourier transform of the diffraction data. A typical result is depicted in fig 4. It shows the density of magnetic moment along 111 plane in the L21 Austenitic phase of the $Ni_{53}Mn_{27}Ga_{20}$ alloy. The data were taken at 340 K under a magnetic field of 2 Tesla, which largely saturates the sample.

The results confirm the previous model in different aspects:

a) Magnetic moments are almost fully localized at Mn atoms in Mn positions (MnMn). Ni positions also show a parallel moment but much lower, as previously assumed. Ga positions show antiparallel magnetic moments arising from the excess Mn atoms located at such positions, coupling antiferromagnetically to the MnMn ones.

b) The average magnetic moment value at Ni positions (NiNi) for the Ni defective alloy is lower than in the other ones. This is expected from the presence of excess Mn atoms at Ni positions, coupling antiferromagnetically with the total moment.

c) MnMn atoms show small average moment values in the excess Ni composition, thus confirming that the excess Ni occupy the Mn positions and decrease the total magnetic moment at the Mn positions, due the lower magnetic moment of the Ni atoms.

d) The average moment of MnGa atoms is smaller in the lowest Ni content alloy. This supports our model of both ferromagnetic and antiferromagnetic coupling of the MnGa atoms depending on the neighbor Ni sites being occupied by Mn atoms or not.

The above findings strongly support the localized model for the magnetism in NiMnGa, and the scheme of FM and AF interactions among Mn atoms as a function of the atomic distance. On the other hand, the magnetic moment per Mn atom deduced from the experiment is different for each alloy, despite the reduced measuring temperature of all of them being the same (T_{meas}/T_{Curie} = 0.92) [22]. This finding can be of great help for first principles calculations of the magnetic moment in such alloys.

As shown, direct determination of the magnetic moment on the crystal positions by PND is a formidable tool to know the magnetic structure of the off stoichiometric NiMnGa FSMAs. However, the complementary knowledge of the site occupation by the different atoms is a previous requirement to interpret the results.

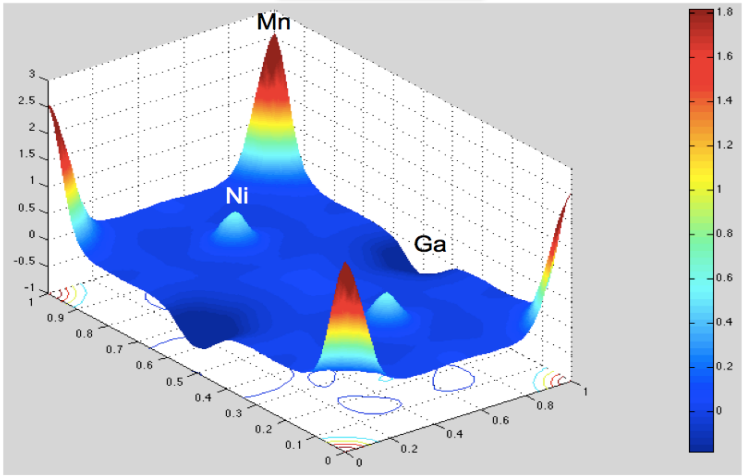

Figure 4. Magnetic moment distribution of Ni53Mn27Ga20 along the 111 plane of the L21 structure as to include all atomic positions. Labeling refers to stoichiometric positions of the corresponding atoms. The magnetic moment is mainly localized at the Mn positions. A much lower value appears at Ni positions, as expected. The negative moment at Ga sites is due to the excess Mn atoms located in such positions.

In the case of FSMAs with more than two magnetic atoms per unit cell, the above procedure is useless, because there are quite a number of possible magnetic moments assigned to each atom that can give results close to each other. A different technique, X rays Magnetic Circular Dichroism (XMCD), gives the magnetic moment of each specific atom, whatever the position in the crystal lattice it occupies, and is more desirable for such compounds.

Recently the determination of the magnetic moment by XMCD has been carried out in a three magnetic component ferromagnetic shape memory alloy (FSMA): $Ni_{49}Fe_{17.5}Co_{4.5}Ga_{29}$ [23]. The sample was prepared in the form of a thin film by sputtering, in order to maximize the volume explored by the

beam using a low incident angle. Atomic moments have been determined at room temperature (Austenite) and at 50K (Martensite), and the results are depicted in fig. 5. The main conclusion is that the three atoms couple FM in both phases and the average moment of each atomic species among all the crystal positions can be obtained independently. This conclusion is really specific of XMCD and couldn't be obtained by neutrons. Both techniques are, therefore, complementary.

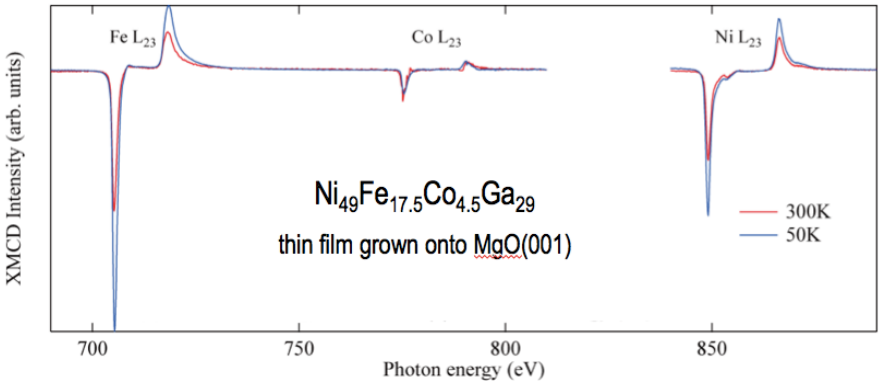

Figure 5. Magnetic Circular Dichroism in a FSMA thin film with three different magnetic atoms in its composition.

A different kind of magnetic shape memory alloys from the NiMnGa discussed before, are those showing Meta-Magnetic behavior (MMSMA). Their composition includes In, Sn or Sb instead of Ga (see, e.g., [24] and references therein). In such alloys the martensite, just below the transformation temperature, has a vanishing saturation magnetization (fig. 6), because of this, the reverse transformation into austenite can be induced by a moderate magnetic field [24-26]. The magnetic character of the martensitic phase is controversial and several options have been proposed, such as spin glass [27, 28], antiferromagnetic [29] or simply paramagnetic [30].

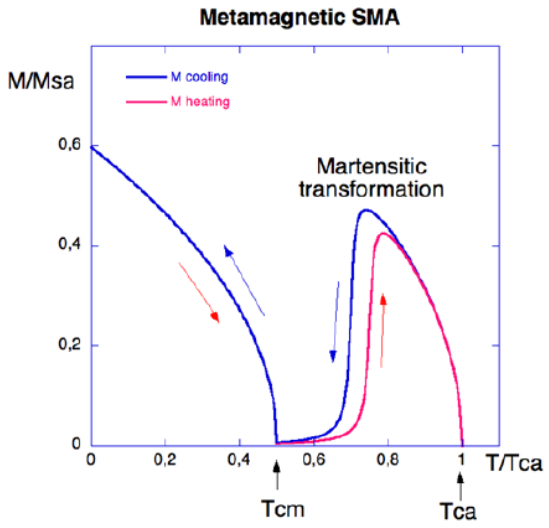

Figure 6. Schematic evolution of the saturation magnetization in a MetaMagnetic Shape Memory Alloy (MMSMA) showing a "non magnetic" state below the martensitic transformation temperature and above the martensitic Curie temperature T_{cm}.

A recent study by XMCD [31] on a MMSMA thin film of composition Ni48Co5Mn35In12, has found an antiparallel alignment of Mn and Ni/Co magnetic moments in both Austenite and Martensite phases. Theoretical first principles calculations agree with the finding. The XMCD reveals itself as a powerful technique that will see an increasing demand in the next years**.**

5. Conclusions

Both neutrons and synchrotron radiation have a great role to play in the study of Magnetic Shape Memory alloys. Inelastic Neutron Scattering is the perfect tool for phonon studies at the structural transformations in SMA and FSMAs, while XPS have a complementary role in determining the electronic mechanisms of the transformation, that has been attributed to a Jahn-Teller distortion. Neutron diffraction is much more powerful than X-rays for superstructure studies and site occupancy determination in NiMnGa alloys, both as a function of composition and thermal treatments, because of the very different scattering lengths for the three atoms. XANES ands EXAFS are complementary to Neutron diffraction to follow the chemical order evolution upon annealing.

Polarized neutron diffraction (PND) experiments allow to determine the localized moment of Ni and Mn atoms in off stoichiometric NiMnGa single crystals, provided site occupancy is simultaneously known. XMCD is complementary to PND for determining the magnetic moment as it is atom specific. In case of more that two magnetic atoms in the structure XMCD is unique in giving a detailed picture of the magnetic coupling.

Acknowledgments

The authors want to thank B. Ouladiaff, C. Mondeli, T. Hansen and A. Stalnaut for assistance in the neutron diffraction measurements at ILL, and J. Chaboy, C. A. Jenkins, N. Kawamura and K. Sumida for XANES and XMCD experiments in Spring 8.

Funding by the Spanish Ministry Economy and Competitiveness (grant MAT2014-56116), the Basque Departments of Industry (ACTIMAT project) and Education (funding of consolidated research groups of the University of the Basque Country) is greatly acknowledged.

References

[1] Webster P J, Ziebeck K R A, Town S L and Peak M S 1984 *Philos. Mag. B* **49** 295
[2] Brown P J, Bargawi A Y, Crangle J, Neumann K-U and Ziebeck K R A 1999 *J. Phys.: Condens. Matter.* **11** 4715
[3] Pons J, Chernenko V A, Santamarta R and Cesari E 2000 *Acta Mater.* **48** 3027
[4] Enkovaara J, Ayuela A, Jalkanen J, NordstroÅNm L and Nieminen R M 2003 *Phys. Rev. B* **67** 054417
[5] Barman S R, Banik S and Chakrabarti A 2005 *Phys. Rev. B* **72** 184410
[6] Chakrabarti A, Biswas C, Banik S, Dhaka R S, Shukla A K and Barman S R 2005 *Phys. Rev. B* **72** 073103
[7] Brown P J, Crangle J, Kanomata T, Matsumoto M, Neumann K-U, Ouladdiaf B and Ziebeck K R A 2002 *J. Phys.: Condens. Matter* **14** 10159
[8] Brown P J, Gandy A P, Kanomata T, Matsumoto M, Neummann K, Neumann K-U, Sheikh A and Ziebeck K R A 2008 *Mater. Sci. Forum* **583** 285
[9] Barandiaran J M, Gutiérrez J, Lázpita P and Feuchtwanger J 2011 *Mater. Sci. Forum* **684** 73
[10] Bacon G E 19777 *Neutron scattering in chemistry* (Butterworths, London and Boston)
[11] 2003 *Neutron data booklet* (Eds. Dianoux A J and Lander G, Institute Laue-Langevin)
[12] Zheludev A, Shapiro S M and Wochner P 1996 *Phys. Rev. B* **54** 15045
[13] Recarte V, Perez-Landazabal J I, Sanchez-Alarcos V, Cesari E, Jimenez-Ruiz M, Schmalz K and Chernenko V A 2013 *App. Phys. Lett.* **102** 201906

[14] Kimura A, Ye M, Taniguchi M, Ikenaga E, Barandiaran J M and Chernenko V A 2013 *Appl. Physics. Lett.* **103** 072403
[15] Gutiérrez J, Barandiarán J M, Lázpita P, Seguí C and Cesari E 2006 *Sensors and Actuators A* **129** 163
[16] Recarte V, Perez-Landazabal J I, Gomez-Polo C, Sanchez-Alarcos V, Cesari E and Pons J 2010 *J. Phys. Condens. Matter* **22** 416001
[17] Chaboy J, Lázpita P, Barandiarán J M, Gutiérrez J, Fernández-Gubieda M L and Kawamura N 2009 *J. Phys.: Condens. Matter.* **21** 016002
[18] Richard M L, Feuchtwanger J, Allen S M, O'Handley R C, Lazpita P, Barandiaran J M, Gutierrez J, Ouladdiaf B, Mondelli C, Lograsso T and Schlagel S 2007 *Phil. Mag.* **87** 3437
[19] Lázpita P, Barandiarán J M, Gutiérrez J, Feuchtwanger J, Chernenko V A and Richard M L 2011 *New Journal of Physics* **13** 033039
[20] Islam A, Haskel D, Lang J C, Srajer G, Lee Y, Harmon B, Goldman A I, Schlagel D L and Lograsso T A 2006 *J. Magn. Magn. Mater.* **303** 20
[21] Lázpita P, Gutierrez J, Barandiaran J M, Chernenko V A, Mondelli C and Chapon L 2014 *J. Phy,: Conf. Series* **549** 012016
[22] Papoular R J and Gillon B 1990 *Europhys. Lett.* **13** (5) 429
[23] Sumida K, Shirai K, Zhu S, Taniguchi M, Ye M, Ueda S, Takeda Y, Saitoh Y, Rodriguez I, Barandiaran J M, Chernenko V A and Kimura A (*to be published*)
[24] Planes A, Manosa Ll and Acet M 2009 *J. Phys.: Cond. Mat.* **21** 233201
[25] Kainuma R, Imano Y, Ito W, Sutou Y, Morito H, Okamoto S, Kitakami O, Oikawa K, Fujita A, Kanomata T and Ishida K 2006 *Nature* **439** 957
[26] Sharma V K, Chattopadhyay M K, Chouhan A and Roy S B 2009 *J. Phys. D: Appl. Phys*. **42** 185005
[27] Cong D Y, Roth S, Liu J, Luo Q, Pötschke M, Hürrich C and Schultz L 2010 *Appl. Phys. Lett.* **96** 112504
[28] Pramanick S, Chattopadhyay S, Giri S, MajumdarS and Chatterjee S 2014 *J. Appl. Phys.* **116** 083910
[29] Liao P, Jing C, Wang X L, Yang Y J, Zheng D, Li Z, Kang B J, Deng D M, Cao S X, Zhang J C and Lu B 2014 *Appl. Phys. Lett.* **104** 092410
[30] Umetsu R Y, Kainuma R, Amako Y, Taniguchi Y, Kanomata T, Fukushima K, Fujita A, Oikawa K and Ishida K 2008 *Appl. Phys. Lett.* **93** 042509
[31] Klaer P, Herper H C, Entel P, Niemann R, Schultz L, Fähler S and Elmers H J 2013 *Phys. Rev. B* **88** 174414